



Research paper

Profiling of cellular immune responses to *Mycoplasma pulmonis* infection in C57BL/6 and DBA/2 miceTussapon Boonyarattanasoonthorn^a, Yaser Hosny Ali Elewa^{b,c}, Hassan T. Tag-El-Din-Hassan^{a,d}, Masami Morimatsu^a, Takashi Agui^{a,*}^a Laboratory of Laboratory Animal Science and Medicine, Department of Applied Veterinary Sciences, Graduate School of Veterinary Medicine, Hokkaido University, Sapporo 060-0818, Japan^b Laboratory of Anatomy, Department of Basic Veterinary Sciences, Graduate School of Veterinary Medicine, Hokkaido University, Sapporo 060-0818, Japan^c Department of Histology and Cytology, Faculty of Veterinary Medicine, Zagazig University, Zagazig 44519, Egypt^d Poultry Production Department, Mansoura University, Mansoura 35516, Egypt

ARTICLE INFO

Keywords:

Mycoplasma pulmonis
Pneumonia
Cellular immune response
Cytokine
Susceptibility
Inbred mouse

ABSTRACT

Mycoplasma infections cause respiratory tract damages and atypical pneumonia, resulting in serious problems in humans and animals worldwide. It is well known that laboratory inbred mouse strains show various susceptibility to *Mycoplasma pulmonis* (*M. pulmonis*) infection, which causes murine respiratory mycoplasmosis. In this study, we aimed to demonstrate the difference in cellular immune responses between resistant strain, C57BL/6NCrSlc (B6) and susceptible strain, DBA/2CrSlc (D2) after challenging *M. pulmonis* infection. D2 mice showed higher amount of bacterial proliferation in lung, higher pulmonary infiltration of immune cells such as neutrophils, macrophages, and lymphocytes, and higher levels of interleukin (IL)-1 β , IL-6, IL-17A, and tumor necrosis factor- α in bronchoalveolar lavage fluid than did B6 mice. The results of this study suggest that D2 mice are more susceptible than B6 mice to *M. pulmonis* infection due to a hyper-immune inflammatory response.

1. Introduction

Mycoplasma infection is a cause of respiratory disease in humans (Waites and Talkington, 2004) and animals. Mycoplasmosis in humans accounts for 20 to 40% of all cases of pneumonia patients in the United States (Waller et al., 2014) and causes macrolide resistance problems (Diaz et al., 2015; Pereyre et al., 2016). In livestock, mycoplasma respiratory infections also causes a huge problem and make a significant economic loss in many countries (Boettger and Dohms, 2006; Calcutt et al., 2018; Luehrs et al., 2017). In addition, many kinds of animals can be infected with mycoplasmas and receive the severe impact from the infection.

Mycoplasma pulmonis (*M. pulmonis*), a pleomorphic bacterium lacking a cell wall, is mainly implicated in murine respiratory mycoplasmosis (Chawla et al., 2017; Ceola et al., 2016; Ferreira et al., 2008) and can be transmitted by airborne droplet of nasopharyngeal secretion. *Mycoplasma* infection in laboratory mouse colonies causes severe problems to respiratory tract associated with rhinitis, otitis media, laryngotracheitis, and bronchopneumonia, leading to significant affects in the result of experiment (Davis et al., 1985). In terms of

histopathology, mycoplasma infections are recognized by the accumulation of mononuclear and polynuclear cells along the respiratory airways (Cartner et al., 1996; Davidson et al., 1988). Previous studies with different inbred mouse strains showed various susceptibility to this bacterial infection. For instance, infected C57BL/6 (B6) mice have bacterial load in their lungs 100–100,000 times lower than infected C3H mice (Cartner et al., 1995) as well as lower gross lung lesions and lung histopathological lesions. However, the information mentioned above was mainly investigated in B6, C3H and BALB/c mice (Davidson et al., 1988; Hickman-Davis et al., 1997; Lai et al., 1996; Sun et al., 2006). For DBA/2 (D2) mice very limited information is available and cellular immune responses are unknown. The results from our preliminary experiment among three inbred mouse strains, B6, C3H and D2 mice exhibited that B6 and D2 mice were the most different in symptoms caused by *M. pulmonis* infection. Therefore, it is critical to determine the mechanisms of immune responses that contribute to mycoplasmosis. This information may contribute to the development of new vaccines and comprehensive knowledge for mycoplasmosis. Both of innate and adaptive immune responses are associated with disease severity and susceptibility between the strains of mice (Davis et al.,

* Corresponding author at: Laboratory of Laboratory Animal Science and Medicine, Department of Applied Veterinary Sciences, Graduate School of Veterinary Medicine, Hokkaido University, Kita 18, Nishi 9, Kita-ku, Sapporo, Hokkaido 060-0818, Japan.

E-mail address: agui@vetmed.hokudai.ac.jp (T. Agui).

<https://doi.org/10.1016/j.meegid.2019.04.019>

Received 29 January 2019; Received in revised form 19 April 2019; Accepted 21 April 2019

Available online 23 April 2019

1567-1348/ © 2019 Elsevier B.V. All rights reserved.

1985). Inflammatory cellular and humoral responses have been used to investigate the host-pathogen interactions in various microbes (Cardona et al., 2003; Lan et al., 2016; Simon et al., 2011; Szczepanek et al., 2012). Differences in the response of immune cells and cytokines may be attributed to resistance or susceptibility in mice to mycoplasma infection.

Thus, in the current study, we examined the cellular immune responses by using two inbred mouse strains, B6 (resistant) and D2 (susceptible), to exhibit the profiling of the infection by observing disease-associated phenotypes such as lung histopathological lesions, propagation of bacteria in lung, lung cytological changes, cytokines levels in bronchoalveolar lavage fluid (BALF), and areas of lymphoid clusters (LCs) in mediastinal fat tissues (MFTs). Furthermore, we performed quantitative trait locus (QTL) analysis using these infected phenotypes as QTs to dissect genetic factors regulating the difference between these two inbred strains. We found that D2 mice constantly had much greater number of CFU of *M. pulmonis* in their lung, greater severity of lung lesions, higher pulmonary infiltration of immune cells, and higher levels of cytokines in BALF. This study first examined and compiled the cellular immune responses from *M. pulmonis* infection in B6 and D2 mice. The results suggest that D2 mice are more susceptible than B6 mice to *M. pulmonis* infection due to a hyper-immune inflammatory response.

2. Materials and methods

2.1. Mice

Specific pathogen-free (SPF) 8-week-old female and male C57BL/6NcrSlc (B6) and DBA/2CrSlc (D2) mice were purchased from Japan SLC (Hamamatsu, Japan). All animals were kept under SPF conditions and infection experiments were conducted in the bio-safety level 3 facilities with sterile food and water *ad libitum*. Animal experimentation was conducted under the AAALAC International-accredited program and animal use protocol was approved by the President of Hokkaido University after review by the Institutional Animal Care and Use Committee.

2.2. Bacteria and infection

The CIEA-NH strain of *M. pulmonis* was kindly provided by Dr. Nobuhito Hayashimoto, Central Institute for Experimental Animals, Japan. Mycoplasma broth was made as follows; 21 g of mycoplasma broth base (BBL Microbiology Systems, Cockeysville, MD, USA), 5 g of D (+) -glucose (Wako Pure Chemical Industries, Ltd., Osaka, Japan), and 20 mg of phenol red (Wako) were dissolved with 750 ml of distilled water, autoclaved for 15 min, allowed to cool, and then 150 ml of heat-inactivated horse serum (GIBCO Laboratories, Grand Island, NY, USA), 100 ml of 25% fresh yeast extracts (Oriental Yeast Co., Ltd., Tokyo, Japan), 10 ml of 2.5% thallium acetate (Wako), and 1000,000 units of ampicillin sodium salt (Sigma Chemical Company, Saint Louis, MO, USA) were added. After propagating *M. pulmonis* in the above broth, the stock cultures were divided into 1-ml aliquots and frozen at -80°C until used. Mice from each strain ($n = 5-6$ per time point) were inoculated intranasally with 6.0×10^5 CFU of *M. pulmonis* in 30 μl of inoculum after anesthetization with inhalation of isoflurane (Escain®; Pfizer Co., Ltd., Tokyo, Japan) followed by intraperitoneal injection of the mixture of 0.75 mg/kg body weight (b.w.) medetomidine (Domitor® Nippon Zenyaku Kogyo Co., Ltd., Koriyama, Japan), 4.0 mg/kg b.w. midazolam (Dormicum®, Astellas Pharma Inc., Tokyo, Japan), and 5.0 mg/kg b.w. butorphanol (Vetorphale®, Meiji Seika Pharma, Ltd., Tokyo, Japan) (Kawai et al., 2011). Control mice from each strain ($n = 5$ per time point) received the same volume of mycoplasma broth alone after the same anesthetization. Mice were daily observed clinical signs, body temperature, and body weight. The samplings were performed at 7, 14, and 21 days post infection (d.p.i.) after euthanizing

mice by inhalation of overdose of isoflurane (Escain®; Pfizer Co., Ltd.,).

2.3. Quantitative culture of *M. pulmonis* in lungs of infected mice

Mice were euthanized at the indicated time points. Lungs were removed aseptically and homogenized in 1 ml of mycoplasma broth with glass homogenizers (Sankyo Co., Ltd., Tokyo, Japan). Ten-fold serial dilutions were prepared and an aliquot of 10 μl of each dilution was plated onto PPLO agar medium, which was made by dissolving 35 g of PPLO agar (Becton Dickinson and Company, Sparks, MD, USA) with 750 ml of distilled water, autoclaved for 15 min, allowed to cool at $52-54^{\circ}\text{C}$, and then 150 ml of heat-inactivated horse serum (GIBCO), 100 ml of 25% fresh yeast extracts (Oriental Yeast), and 1000,000 units of ampicillin sodium salt (Sigma) were added. The total number of colony-forming unit (CFU) per lung from each animal was determined under a stereomicroscope after incubation for 10 days at 37°C in an incubator with 5% CO_2 .

2.4. Determination of bacterial load by quantitative PCR

The bacterial replication level in the lung was determined by quantitative real-time PCR. Briefly, mice from each group were sacrificed at 7, 14, and 21 d.p.i. and whole lungs were collected by aseptic technique. The individual lung from each mouse was homogenized in 1 ml of mycoplasma broth with glass homogenizers (Sankyo Co., Ltd.). The homogenized lung suspension (300 μl) was used for DNA extraction. DNA was extracted by adding 500 μl of lysis buffer [10 mM Tris (Wako), 10 mM ethylenediaminetetraacetic acid (EDTA)-2Na (Wako), 150 mM NaCl (Wako), and 0.1% sodium dodecyl sulfate (Wako)] and 5 μl of 10 mg/ml proteinase K (Invitrogen, Carlsbad, CA, USA) and incubating for 3–4 h at 54°C for lysis. To detect *M. pulmonis* DNA, total DNA was used as a template with PCR primers, which were designed based on the conserved spacer region encompassing the 16S and 23S rRNA gene of *M. pulmonis* (Harasawa et al., 2005; Loganbill et al., 2005; Takahashi-Omoe et al., 2004). The primers used were FN2 (5'-ACCTC CTTTCTACGGAGTACAA-3') and R2 (5'-GCATCCACTACAACTCTT-3') (Sung et al., 2006). Quantitative real-time PCR was performed using the FastStart Essential DNA Green Master (Roche Diagnostics Corporation, Indianapolis, IN, USA) and LightCycler96 instrument (Roche). A reaction mixture (10 μl) contained 1 μM of each primer, 5 μl of FastStart Essential DNA Green Master (Roche), and 50 ng of genomic DNA template. Amplification conditions consisted of 45 cycles of denaturation at 95°C for 10 s, annealing at 60°C for 10 s, and extension at 72°C for 30 s. The products were analyzed with the accompanying software and the amount of bacterial DNA in each sample was calculated using a standard curve, which was plotted serial ten-fold dilutions of template with known concentration.

2.5. Histopathological analysis

Whole lungs and mediastinal fat tissue (MFT) from individual mouse were removed, and then fixed in 4% paraformaldehyde to inflate and preserve lung architecture. After overnight fixation, specimens were washed in distilled water followed by dehydrated in graded alcohol and embedded in paraffin. The paraffin-embedded specimens were sectioned at a thickness of 3 μm , and subsequently deparaffinized, rehydrated, and stained with hematoxylin and eosin (H&E) to observe under a light microscope and examined lesion severity. For lung, ten sections were cut and five fields were randomly observed in each slide. The degree of distribution and severity of inflammatory infiltration/structural alterations were determined on the basis of the characteristic lesions of mycoplasmosis examined around small airways and adjacent blood vessels. Scores (scale of 1 to 6) refer to normal, 1; slight/mild, 2; moderately, 3; severe, 4; and highly severe, 6. Pathological scores for the lung sections were averaged and determined as the pathological index.

Immunohistochemical analysis for Gr1 (Ly-6G) and Iba1 was performed in lung tissue of both B6 and D2 mice to detect neutrophils and macrophages, respectively. Immunohistochemical procedures were performed according to Elewa et al., 2010. Briefly, following deparaffinization, heat-induced antigen retrieval was applied using 0.1% pepsin in 0.2 ml HCl at 37 °C for 5 min and 10 mM citrate buffer (pH 6.0) at 105 °C for 20 min. Then, following endogenous peroxidase blocking with 0.3% hydrogen peroxide in absolute methanol at room temperature for 20 min, the sections were incubated with 10% normal goat serum for 1 h at room temperature. Then the sections were incubated overnight with the specific primary antibody, rat anti-Gr1 (R and D system, Minneapolis, USA) or rabbit anti-Iba1 (Wako, Osaka, Japan), diluted in phosphate-buffered saline (pH 7.2) (PBS) containing 1.5% bovine serum albumin, at dilution of 1:800 or 1:1,200, respectively. Then the sections were incubated with biotin-conjugated secondary antibody, goat-anti-rat IgG for rat anti-Gr1 or goat-anti-rabbit IgG for rabbit anti-Iba1, for 1 h at room temperature, then with streptavidin-peroxidase for 30 min. Between the various steps, sections were thoroughly rinsed in PBS 3 times for 5 min each. The immunopositive reactions were visualized with 3,3'-diaminobenzidine-H₂O₂ solution for 2 min. Then the sections were washed in distilled water, lightly stained with Mayer's hematoxylin for 30 s, dehydrated, and mounted. All sections were photographically captured using the BZ-X710 (Keyence, Osaka, Japan).

For MFT, the light micrographs of H&E-stained MFT sections from each mouse were scanned using a NanoZoomer-XR Digital slide scanner (Hamamatsu Photonics K.K., Hamamatsu, Japan). The area of lymphoid cluster (LC) and the total areas of the mediastinal white adipose tissue within the MFT were measured using NDP.view2 Viewing software (ver. 2.6.13, Hamamatsu Photonics) and the ratio of LC area to total MFT area was calculated.

2.6. Brochoalveolar lavage fluid (BALF) collection and cytology

Mice were euthanized by inhalation of overdose of isoflurane at the indicated time point and BALF was collected as described previously (Daubeuf and Frossard, 2012). Briefly, a sterile 20-gauge animal feeding needle (Fuchigami Instruments Co., Ltd., Kyoto, Japan) was inserted through the mouth and larynx into the lumen of the trachea. The lungs were then slowly lavaged *in situ* with three separated 300 µl of sterile PBS, pH 7.2. The BALF was centrifuged at 300 × g at 4 °C for 5 min, and then the supernatants were collected and stored at –80 °C for the cytokine analysis. The cell pellet was suspended in 1.5 ml of distilled water, placed for 10 s, and then added 500 µl of 0.6 M KCl and mixed by inverting. Suspensions were centrifuged at 300 × g at 4 °C for 5 min and the supernatants were discarded. The cell pellets were re-suspended by adding 500 µl of sterile saline (0.9% NaCl) with 2.6 mM EDTA and mixed by inverting, and then total count of viable leukocytes was determined by using a hemacytometer (Erma Inc., Tokyo, Japan). To determine differential cell count, 200 µl of the BALF cell suspensions were loaded onto a Shandon™ EZ Single Cytofunnel (Thermo Fisher Scientific, Cheshire, UK) and centrifuged for 10 min at 108 × g. Finally, the slides were dried at room temperature and stained with a Diff-Quick Staining Kit according to the manufacturer's protocol.

2.7. Cytokine analysis

A Bio-Plex Pro Mouse Cytokine Th17 Panel A 6-Plex (Bio-Rad, Hercules, CA, USA) was used to evaluate the cytokine levels in BALF supernatant. Interferon (IFN)- γ , interleukin (IL)-1 β , IL-6, IL-10, IL-17A and tumor necrosis factor (TNF)- α were measured according to the manufacturer's protocol. Concentration of each cytokine was determined and calculated using a beads assay on the Bio-Rad Bio-Plex 200 System (Bio-Rad) and Bio-Plex Manager version 6.0 software, respectively.

2.8. Genotyping of microsatellite markers

Extraction of genomic DNA from tail clips was performed by the standard methods. A total of 125 microsatellite markers showing polymorphisms between B6 and D2 mice were used for genetic study as described previously (Simon et al., 2009). The map positions of microsatellite loci were based on information from the Mouse Genome Informatics (MGI; <http://www.informatics.jax.org>). PCR was carried out on a Bio-Rad PCR thermal cycler (iCycler, California, USA) with the cycling sequence of 95 °C for 1 min (one cycle), followed by 35 cycles consisting of denaturation at 95 °C for 30 s, primer annealing at 58 °C for 30 s, and extension at 72 °C for 30 s. PCR mixture and enzymes (*Ex Taq* DNA Polymerase) were purchased from TaKaRa (Otsu, Japan). The amplified samples were electrophoresed with 10–15% polyacrylamide gel (Wako, Osaka, Japan), stained with ethidium bromide, and then photographed under an ultraviolet lamp.

2.9. QTL analysis

One hundred twenty one F₂(B6 x D2) mice were produced, infected with *M. pulmonis* at 8 weeks old, and measured body weight change, CFU of *M. pulmonis* in the lung, and total cells, neutrophils, macrophages, and lymphocytes in infiltrated in BALF as QT at 21 d.p.i. QTL analysis was performed with Map Manager QTXb20 software program (Manly et al., 2001). In this program, linkage probability was examined by interval mapping. For each chromosome, the likelihood ratio statistic (LRS) values were calculated by 5000 random permutations of the trait values relative to genotypes of the marker loci and converted to logarithm of the odds (LOD) score.

2.10. Statistical analysis

The results of the various groups were compared by using an analysis of variance (ANOVA). We used Scheffe's post-hoc test for multiple comparisons when a significant difference was observed by ANOVA ($P < 0.05$). All values were represented as mean \pm standard error (SE). Values of $P \leq 0.05$ were considered statistical significance.

3. Results

3.1. Disease severity and development of lung pathology in infected B6 and D2 mice

To characterize the development of mycoplasmosis in B6 and D2 mice, age- and sex-matched mice of each strain were infected with *M. pulmonis*, and then body weight loss and histological change were evaluated ($n = 5–6$ per time point) at 7, 14, and 21 d.p.i. As a control group, mice were inoculated with mycoplasma broth only. *M. pulmonis*-infected D2 mice showed significant decline in weight ($P < 0.05$) at 7 d.p.i. compared to infected B6 mice as well as broth-inoculated control mice (Fig. 1). Namely, D2 mice exhibited severe body weight loss, nearly 30% from the initial body weight.

In the pathological examination, lungs were collected from infected B6, D2, and broth-inoculated control mice at 7, 14, and 21 d.p.i. Pathological changes were examined through H&E staining of lung sections. D2 mice but not B6 mice distinctly showed gross lung lesions following *M. pulmonis* infection. The gross lesions in infected D2 mice showed moderate to severe pulmonary hemorrhage and consolidation (Fig. 2). The histopathological lesion was suppurative bronchopneumonia with squamoid changes of the respiratory epithelium. Prominent cuffing of bronchi, bronchioles and blood vessels by lymphoid cells as well as parenchymal lesions consisting of alveoli filled with neutrophils and macrophages were common in most of infected D2 mice at all time points (Fig. 3A, B, and C). On the other hand, infected B6 mice showed limited lesions with a few lymphoid cells around the vessels and airways. Infected D2 mice had extensive lymphoid infiltrates such as

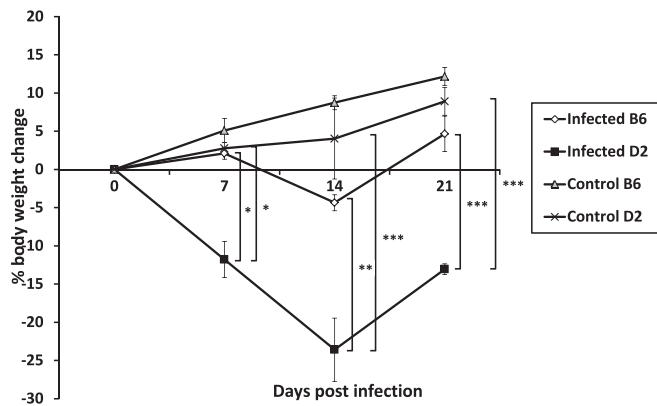


Fig. 1. Body weight changes in infected female B6, infected female D2, and control female mice after *M. pulmonis* infection. The time course of changes was shown in percentage of body weight loss in mice ($n = 5-6$ per group) infected with 6×10^5 CFU of *M. pulmonis*. *, ** and *** indicates $P < 0.05$, $P < 0.01$, and $P < 0.005$, respectively.

macrophages and neutrophils around bronchi, and mixed inflammatory response in alveoli (Fig. 3B and C). These differences included increased exudate, epithelial hyperplasia, and lymphoid hyperplasia in the lungs. There was no difference observed between males and females in both strains (Supplementary Figs. 1 and 2).

The inflammatory dynamics of the pulmonary epithelium were investigated by comparing lung histopathological changes after bacterial infection. The representative histopathology sections taken from each group of mice demonstrated the relative degree of pathological changes that developed in the lungs after the infection. The lung pathological

index scores were significantly higher ($P < 0.01$) in infected D2 mice than in infected B6 mice at all time points (Fig. 3D) and there was no sexual difference (Supplementary Fig. 2).

The stereomicroscopic observation of the MFTs were examined. The result from all mice showed dark-stained regions that varied in shape and size and these regions were confirmed as LCs by subsequent histological examination (Fig. 4A). Especially, the MFTs of infected B6 mice had a smaller number of LCs compared with infected D2 and broth-inoculated control mice at 14 and 21 d.p.i. These observations were confirmed by image viewing. The ratios of LC area to total MFT area in infected B6 mice were not significantly higher than infected D2 mice at 7 d.p.i. but significantly lower ($P < 0.005$) than infected D2 mice at 14 and 21 d.p.i (Fig. 4B).

3.2. Cytology in BALF of infected B6 and D2 mice

Cytology was performed using the suspension of BALF samples from each time point. The number of infiltrated cells was higher in infected D2 than in infected B6 and broth-inoculated control mice at all time points (Fig. 5). After counting the number of each cell type, it was revealed that the total cell counts in infected D2 mice were significantly higher ($P < 0.005$) than in infected B6 and broth-inoculated control mice at all time points (Fig. 6A). For the differential cell count, infected D2 mice had a higher population of neutrophils (Fig. 6B) and macrophages (Fig. 6C) compared with infected B6 ($P < 0.05$) and broth-inoculated control mice ($P < 0.01$). However, lymphocyte population was not significantly different among infected B6, infected D2, and broth-inoculated control mice (Fig. 6D).

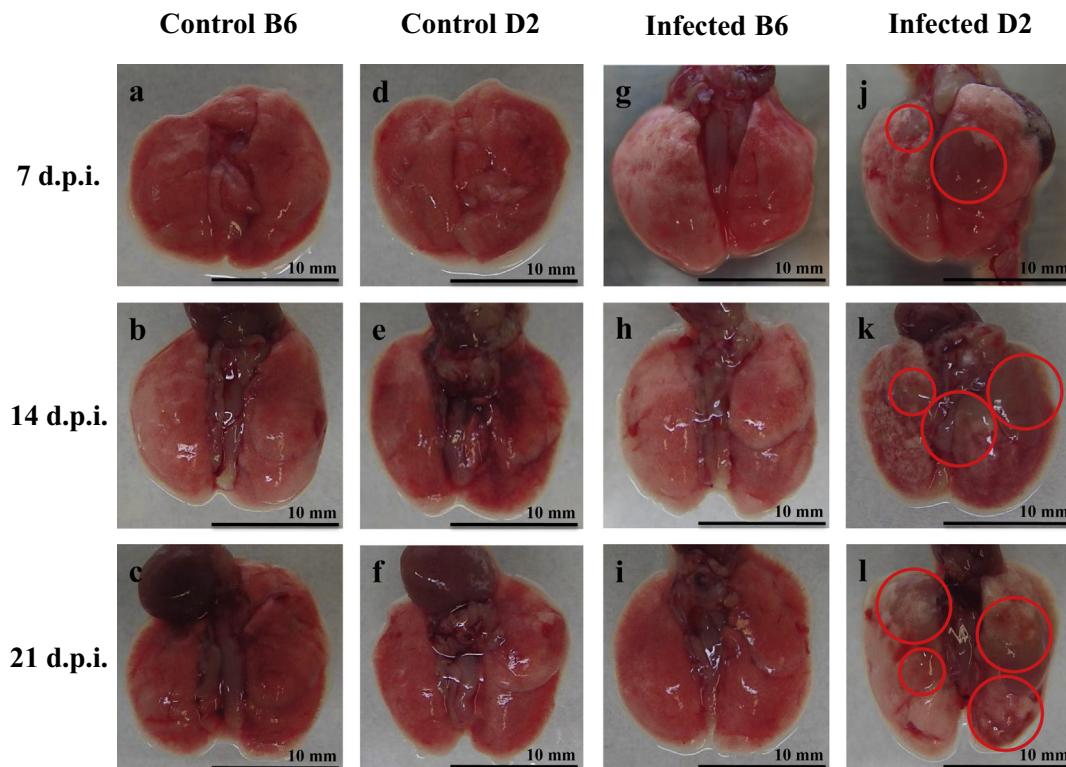
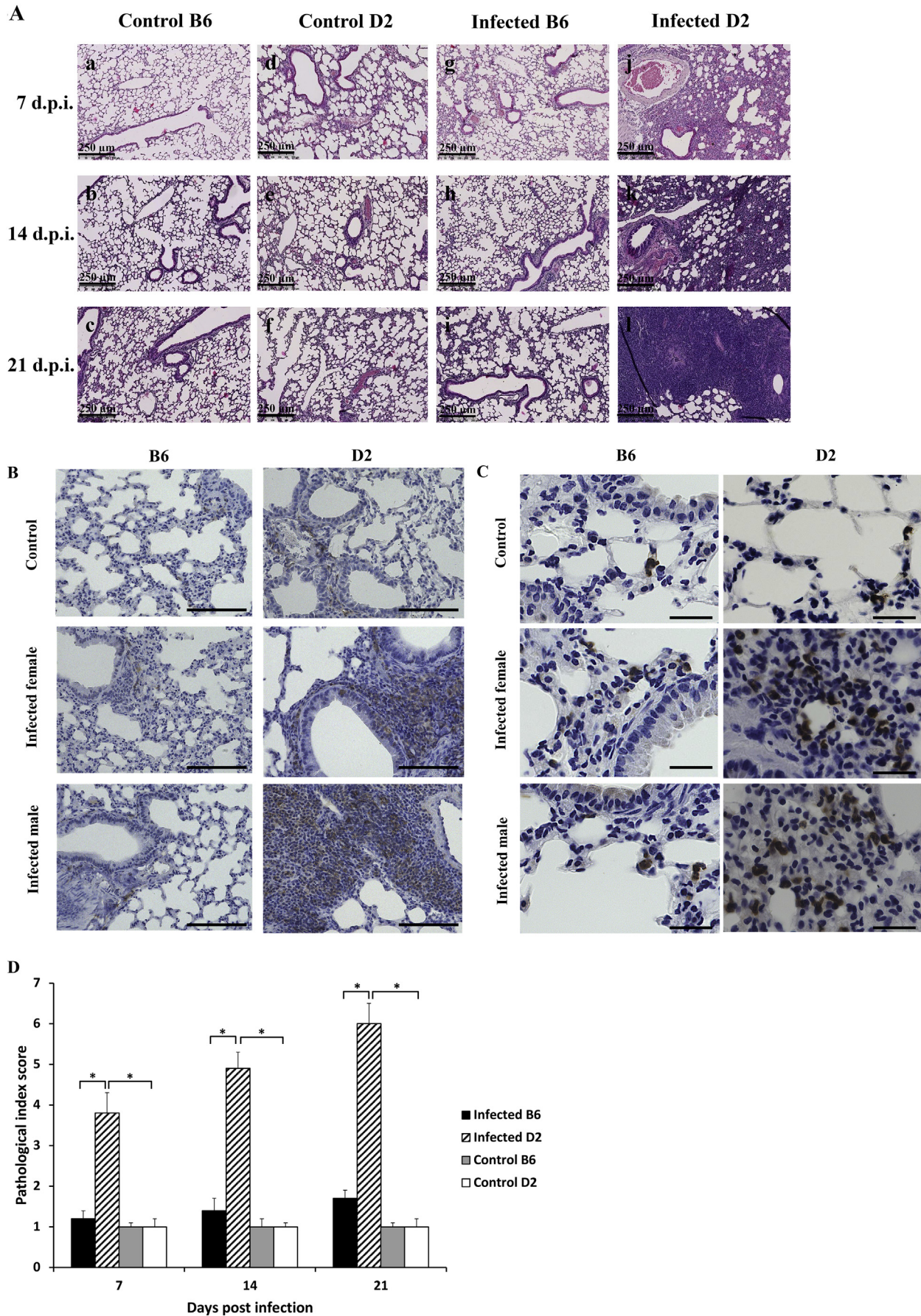


Fig. 2. Gross lung lesions in infected female and control female mice after *M. pulmonis* infection. Results are shown as representatives at each time point ($n = 5-6$ per group) of lungs from control B6 (a-c), control D2 (d-f), infected B6 (g-i), and infected D2 (j-l) mice. Infection was performed using 6×10^5 CFU of *M. pulmonis*. Infected D2 mice showed severe pulmonary hemorrhage and consolidation (red circles in j-l) at all time points. In contrast, no gross lung lesions were observed in control B6, control D2, and infected B6 mice. All scale bars indicate 10 mm. (For interpretation of the references to colour in this figure legend, the reader is referred to the web version of this article.)



(caption on next page)

Fig. 3. (A) Histopathological observation of lung sections in infected female and control female mice after *M. pulmonis* infection. Results are shown as representatives of light microscopic images of H&E-stained lung sections collected from control B6 (a-c), control D2 (d-f), infected B6 (g-i), and infected D2 (j-l) mice (n = 5–6 per group) at the indicated time points after infection with 6×10^5 CFU of *M. pulmonis*. Infected D2 mice (j-l) showed extensive lymphoid infiltration around bronchi, neutrophils in lumen of airways, and mixed inflammatory response in alveoli. Infected B6 mice (g-i) showed lesions limited to a few lymphoid cells around the vessels and airways. The lungs of control mice (a-f) showed mild lymphoid cell infiltration around the vessel and airways. All scale bars indicate 250 μ m. (B) Immunohistochemical staining of Iba1 (macrophage marker) in the lung after two weeks of *M. pulmonis* infection. Infected D2 mice showed numerous Iba-positive cells (stained brown). All scale bars indicate 100 μ m. (C) Immunohistochemical staining of Gr1 (neutrophil marker) in the lung after two weeks of *M. pulmonis* infection. Infected D2 mice showed numerous Gr1-positive cells (stained brown). All scale bars indicate 30 μ m. (D) Lung pathological index score in infected female B6, infected female D2, and control female mice after *M. pulmonis* infection. The histogram showed the pathological index score of lung lesions by H&E staining in each group at the indicated time points. Results are expressed as the mean \pm SE. * indicates $P < 0.01$. (For interpretation of the references to colour in this figure legend, the reader is referred to the web version of this article.)

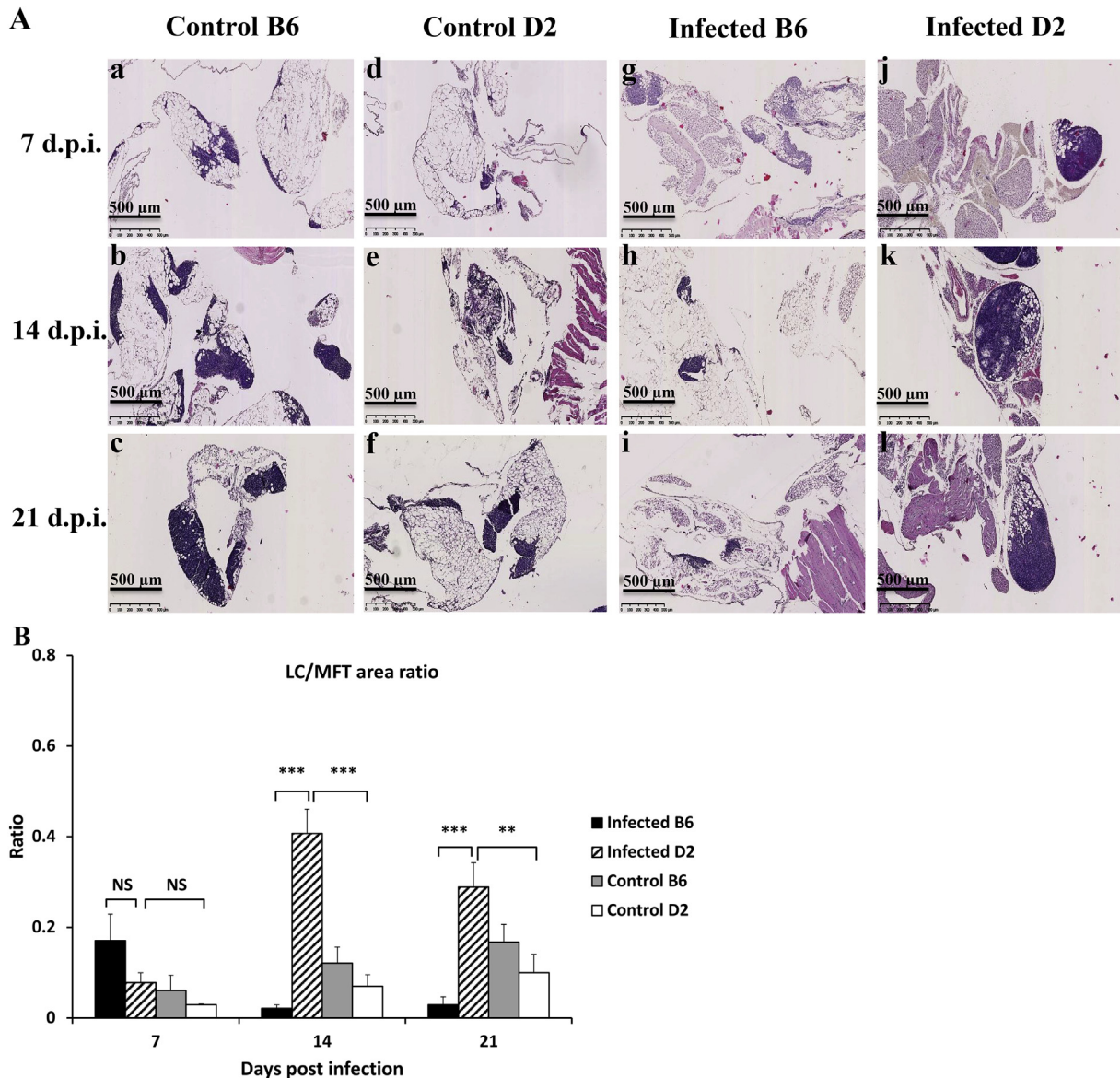


Fig. 4. (A) Histological features of LCs in MFT in infected female and control female mice after *M. pulmonis* infection. Representative light micrographs of H&E-stained MFT sections of control B6 (a-c), control D2 (d-f), infected B6 (g-i), and infected D2 (j-l) mice (n = 5–6 per group) collected at the indicated time points after infection with 6×10^5 CFU of *M. pulmonis*. The accumulation of mononuclear cells is visible in the MFT. Larger areas of LCs are visible in infected D2 mice (j-l) compared with infected B6 (g-i) and control mice. All scale bars indicate 500 μ m. (B) Percentage of LC area in the total MFT area in the H&E-stained sections in infected female B6, infected female D2, and control female mice after infection with 6×10^5 CFU of *M. pulmonis*. Results are expressed as the mean values of the ratio in the experimental groups. ** and *** indicate $P < 0.01$ and $P < 0.005$, respectively. NS; not significantly different.

3.3. Quantification of bacteria in lungs of infected B6 and D2 mice

To determine whether the burden of infection corresponded with disease severity, the numbers of bacteria were determined in the lungs

of mice. There were significant differences in the number of bacteria recovered from the lung between infected B6 and D2 mice (Fig. 7A). At 7 and 14 d.p.i., infected D2 mice had higher ($P < 0.01$) CFU per lung 10^2 - to 10^4 -fold more than infected B6 mice. However, at 21 d.p.i., the

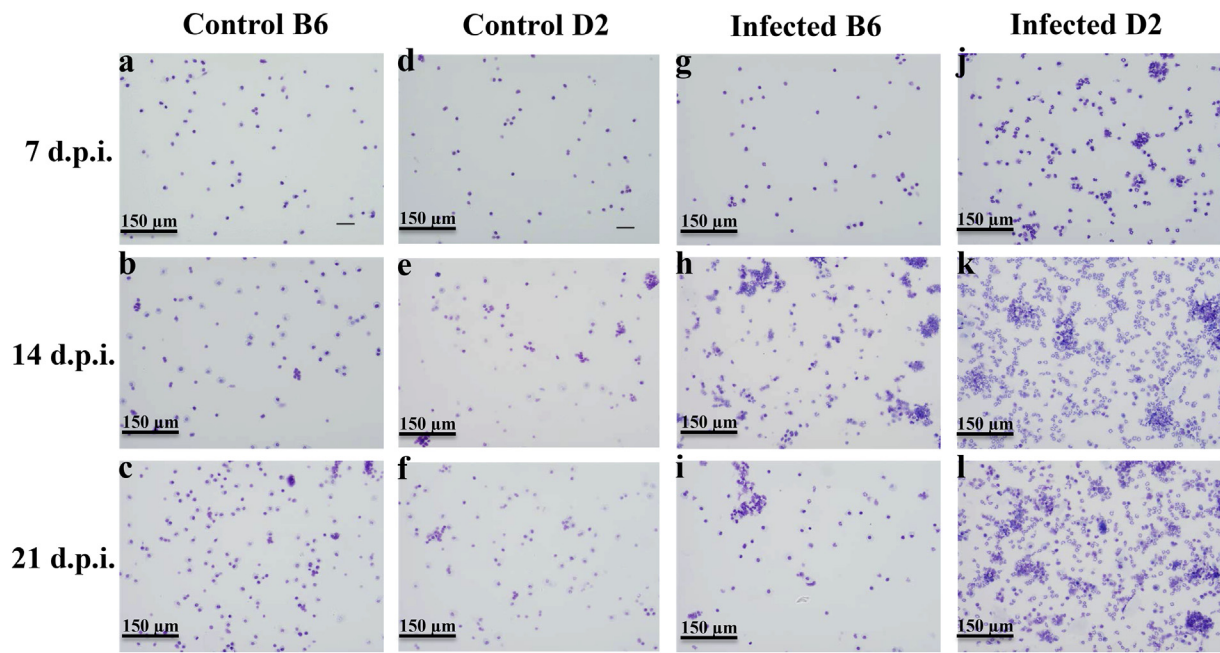


Fig. 5. Cell cytology slides from BALF in infected female and control female mice after *M. pulmonis* infection. Results are shown as representative photomicrographs of Diff-Quick- stained cytospin slides of control B6 (a-c), control D2 (d-f), infected B6 (g-i), and infected D2 (j-l) mice (n = 5–6 per group) at the indicated time points after infection with 6×10^5 CFU of *M. pulmonis*. The accumulation of mononuclear cells is visible in the slide. More inflammatory cells infiltrated are visible in infected D2 mice (j-l) compared with infected B6 (g-i) and control mice. All scale bars indicate 150 μ m.

CFU per lung was not statistically different between infected B6 and D2 mice. Next, we determined the quantity of *M. pulmonis* DNA in lung by quantitative real-time PCR. Infected D2 mice also showed higher ($P < 0.01$) amount of bacterial DNA in lung than infected B6 mice (Fig. 7B). These results affirmed that the D2 mouse was the susceptible strain to *M. pulmonis* infection. The number of bacteria recovered from lung tissues was not different with the sex at the indicated time points (Supplementary Fig. 3).

3.4. Cytokine level in BALF of infected B6 and D2 mice

To exhibit the inflammatory response in lung to the mycoplasma infection, we measured cytokine levels in the supernatant of BALF. The infection induced the expression of pro- and anti-inflammatory cytokines in the lung (Fig. 8). At 7 d.p.i., IL-1 β , IL-6, and TNF- α levels in infected D2 mice were significantly higher ($P < 0.05$) than in infected B6 mice. IL-17A level in infected D2 mice was higher with high

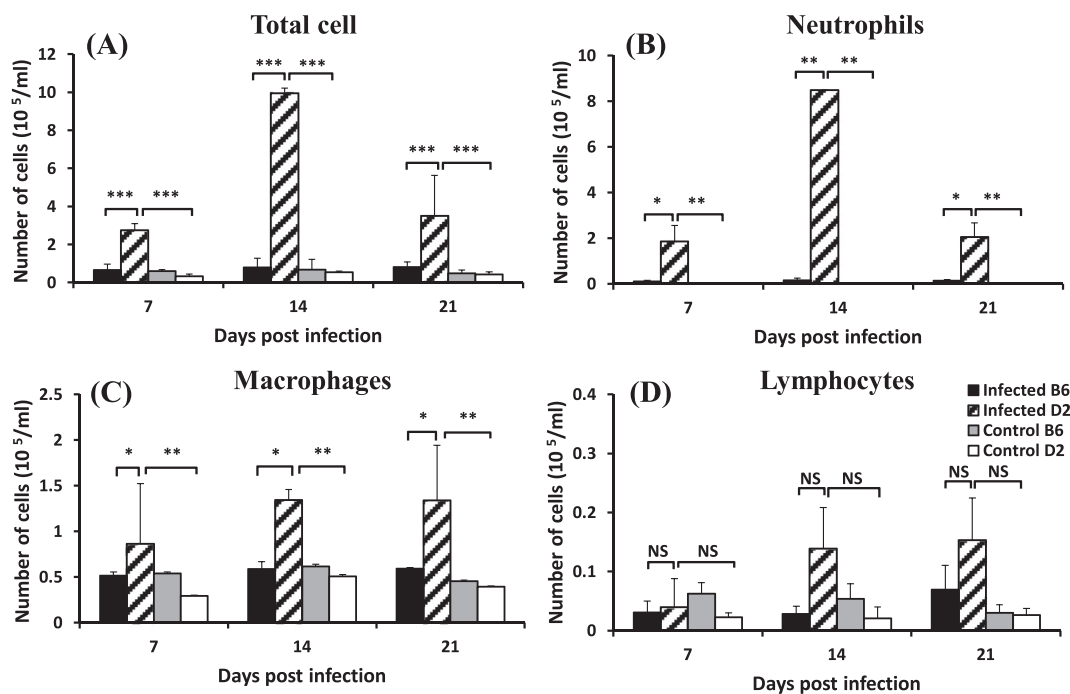


Fig. 6. Total and differential white blood cell counts in BALF in infected female B6, infected female D2, and control female mice after *M. pulmonis* infection. (A), total cells; (B), neutrophils; (C), macrophages; and (D), lymphocytes. Results are expressed as the mean cell counts of the data (n = 5–6 per group). *, **, and *** indicate $P < 0.05$, $P < 0.01$, and $P < 0.005$, respectively. NS; NS; not significantly different.

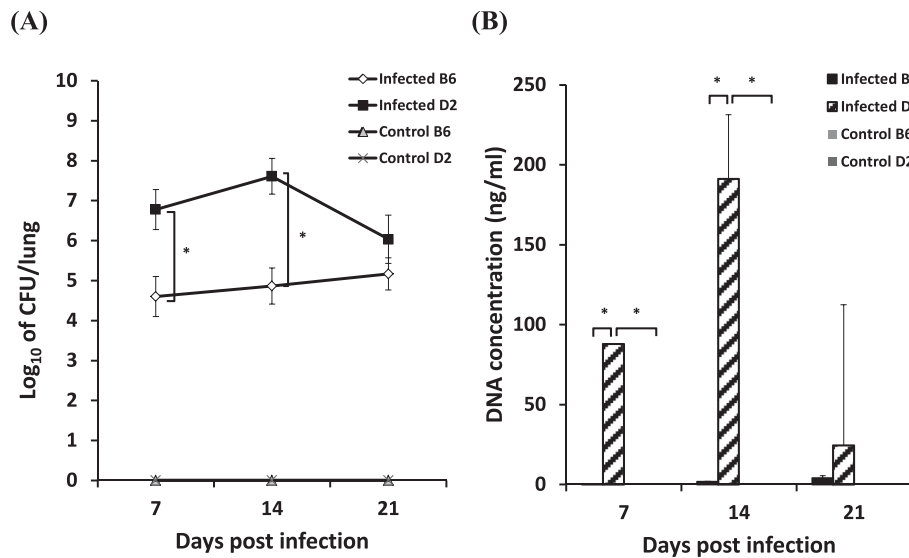


Fig. 7. Amounts of *M. pulmonis* in lungs of infected female B6, infected female D2, and control female mice after *M. pulmonis* infection. (A) CFU of *M. pulmonis* in the culture of whole lung homogenates. (B) *M. pulmonis* DNA concentrations in the homogenized lungs determined by real-time PCR. * indicates $P < 0.01$.

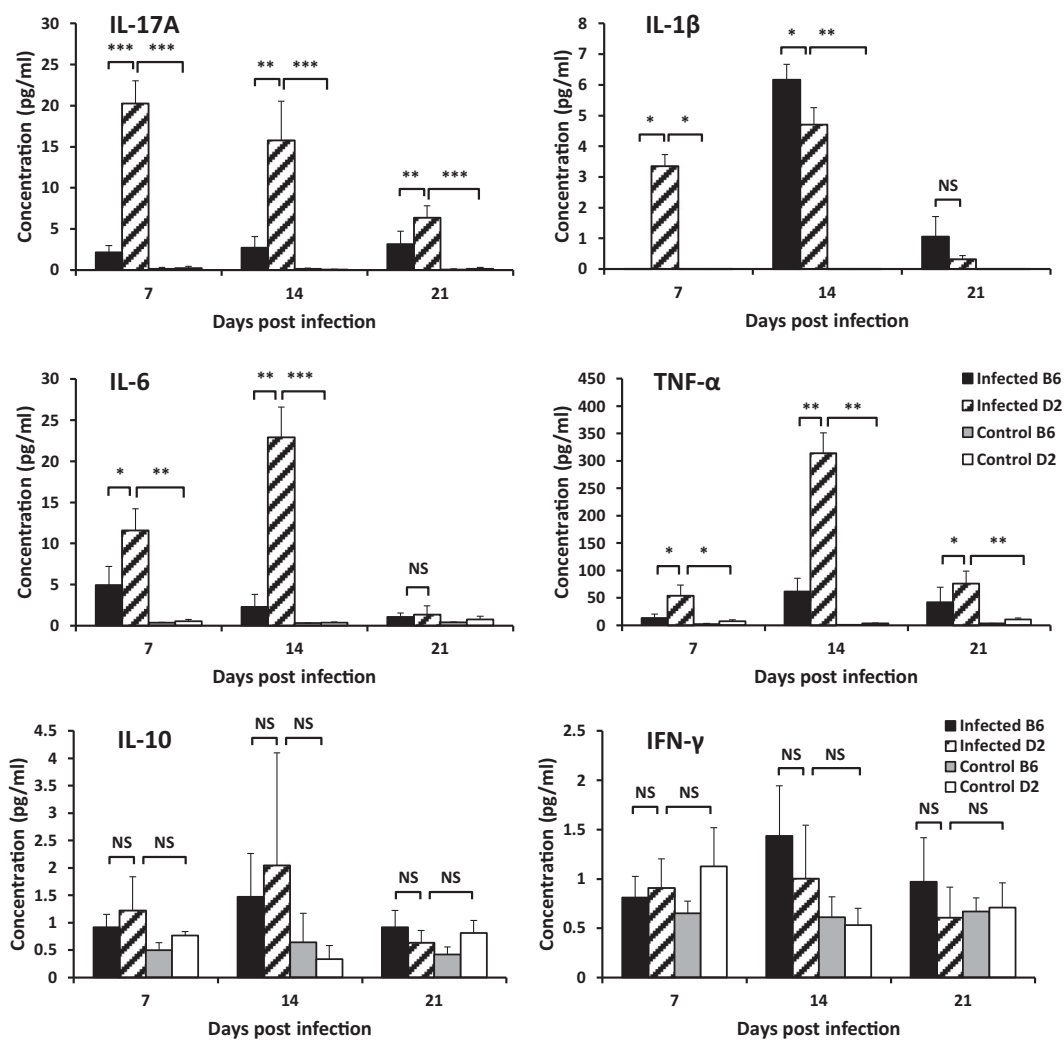


Fig. 8. Pulmonary cytokine levels in infected female B6, infected female D2, and control female mice after *M. pulmonis* infection. Cytokine concentrations in BALF were determined by the Luminex bead assay. Results are expressed as the mean values of samples ($n = 5-6$ per group). Marks of the columns are in common with each small figure. *, **, and *** indicate $P < 0.05$, $P < 0.01$, and $P < 0.005$, respectively. NS; not significantly different.

significance ($P < 0.005$) compared with infected B6 mice. Remarkably, at 14 d.p.i. IL-6, IL-17A, and TNF- α levels were significantly higher ($P < 0.01$) in infected D2 mice compared with infected B6 mice. In contrast, the level of IL-1 β in infected B6 mice was significant higher ($P < 0.05$) than in infected D2 mice. Interestingly, at 21 d.p.i. TNF- α and IL-17A levels in infected D2 mice were significantly higher ($P < 0.05$ and $P < 0.01$, respectively) than infected B6 mice. Moreover, the IL-17A level exhibited the highest level at 7 d.p.i. and declined at 14 and 21 d.p.i. The results confirmed that specific cytokine levels correlate with the bacterial load in lung of infected mice. Nevertheless, in this analysis we did not observe any significant elevation of IL-10 and IFN- γ in infected B6 and D2 mice and found that the level of both cytokines was similar to the normal baseline level of broth-inoculated control mice (Fig. 8).

3.5. QTL analysis

To dissect genetic factors regulating susceptibility or resistance to the *M. pulmonis* infection between B6 and D2 mice, we performed QTL analysis. We selected body weight change, CFU of *M. pulmonis* in the lung, and total cells, neutrophils, macrophages, and lymphocytes in infiltrated in BALF as QTs. Detected QTLs were different each other dependent on QTs used (Fig. 9 and Supplementary Fig. 4). Only when used body weight change as QT, we obtained a significant QTL on chromosome 4 (Fig. 9). These data suggest that the difference in each phenotype between infected B6 and D2 is attributed to different genetic factors.

4. Discussion

The host-pathogen interplay is related to many factors. The genetic background of the animal is one of the important factors that control an immune response. In several infectious diseases, it has been demonstrated that the different strains of animals show different susceptibility caused by different immune responses (Cardona et al., 2003; Pica et al., 2011; Simon et al., 2011; Wilson et al., 2007). In laboratory rodents, distinct difference in the response to the bacterial as well as viral infection was found. The B6 mouse was known to be resistant to the Sendai virus infection (Simon et al., 2009) as well as mycoplasma infection (Davis et al., 1985). On the other hand, the D2 mouse is susceptible to the Sendai virus and mycoplasma infection. Various experiments of *M. pulmonis* infection using susceptible and resistant strains of mouse were performed. Previous study showed that B6 and D2 mice were resistant and susceptible strains to mycoplasma infection, respectively (Sun et al., 2006). However, the mechanism of the susceptibility and resistance is still unclear. Furthermore, little is known about the profiling of immune responses. In this study we performed the infection experiment to display the immune responses to the infection including body weight loss, histopathology of lung, bacterial load in lung tissues, cell cytology, and cytokine levels in BALF as well as histology of MFTs. Furthermore, we performed QTL analysis to dissect genetic factors controlling the difference in these phenotypes.

In the present study, we evaluated the disease severity in both susceptible D2 and resistant B6 mice after *M. pulmonis* infection. There was a clear association between disease pathogenesis and the quantity of bacteria recovered from lungs. The susceptible D2 mice distinctly

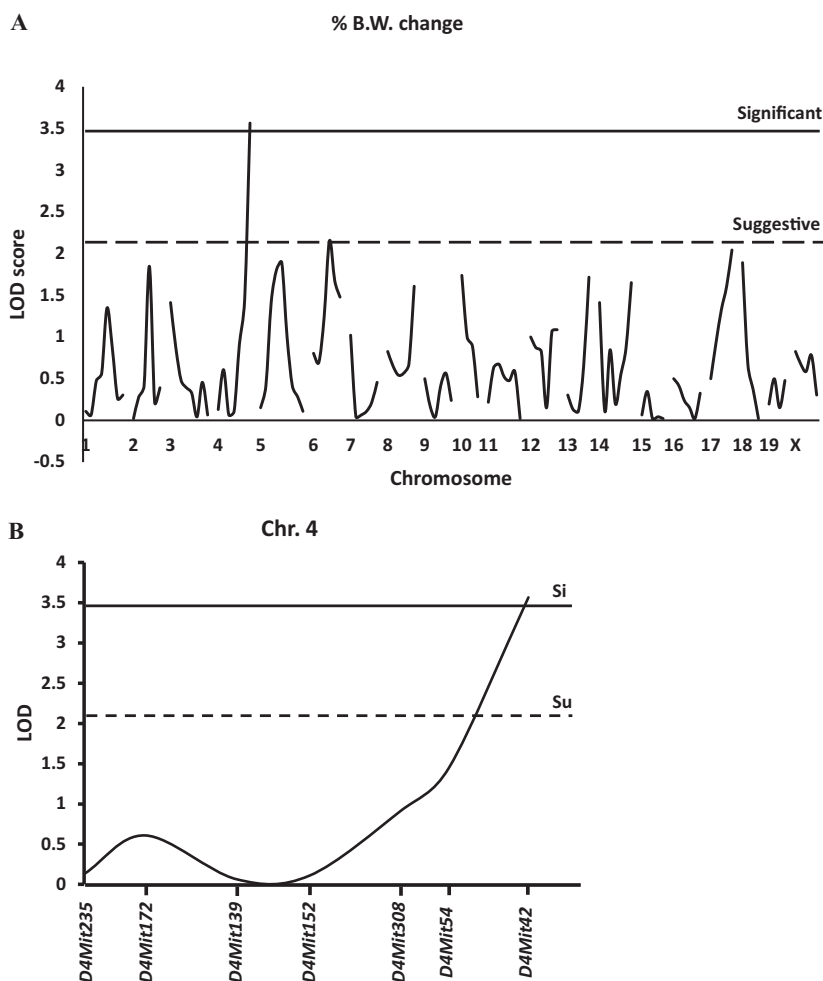


Fig. 9. QTL scan showing LOD score and genome positions associated with the body weight change after *M. pulmonis* infection. (A) The x and y axes show chromosome number and LOD score, respectively. The horizontal lines across the plot indicate two confidence thresholds calculated at 5% (thick, significant) and 63% (dotted, suggestive) level of significance. One significant QTL ($p = 0.00027$) was detected at 151.6 Mbp on chromosome 4 with 3.6 LOD score and one suggestive QTL ($p = 0.00713$) was detected at 75.4 Mbp on chromosome 6 with 2.2 LOD score. (B) Enlarged figure for chromosome 4. The x and y axes show microsatellite marker positions and LOD score, respectively.

expressed gross lung lesions and histologic lung lesions as determined by macroscopic and microscopic examinations after the infection. In contrast, there was a very limited histological lesion in resistant B6 mice. Our results showed that the period of pulmonary immune response to *M. pulmonis* infection in D2 mice was early and intense (Fig. 2 and Fig. 3) consistent to the result of cytokine levels and bacterial load in lung as reported previously (Cartner et al., 1996; Sun et al., 2006). The results from the CFU counting were highly correlated with data obtained by quantitative real-time PCR. The number of *M. pulmonis* recovered from lungs in D2 mice was 1000 times higher than that from B6 mice (Fig. 7). Bacterial burden may cause proinflammatory cytokine induction and result in the strain difference in the severity of the infection. *M. pulmonis* infection strongly induced cytokines such as IL-1 β , IL-6, TNF- α with their peak observed at 14 d.p.i., and IL-17A level with its peak at 7 d.p.i., while other cytokines did not differ significantly between infected and control mice (Fig. 8). It has been reported that IL-1 β , IL-6, and TNF- α augment IL-17A production (Miossec et al., 2009; Chen et al., 2013). Our results are consistent to these previous reports. The elevation of these cytokines may contribute to the exacerbated disease observed in D2 mice. The high expression of these cytokines was consistent with the recruitment of inflammatory cells, including neutrophils, macrophages, and lymphocytes to the lung of infected mice. The over induction of these cytokines in D2 mice might cause the over response to the infection and resulted in excessive inflammatory reaction that can be observed in the histopathological sections of lung tissues (Fig. 3). Interestingly, B6 mice showed significant increase in IL-1 β level higher than D2 mice at 14 d.p.i. (Fig. 8), and it may result in efficient control of inflammation by reducing cytokine production (Vogels et al., 1994, 1995) and blocking of the bacterial growth in lung (Sahoo et al., 2011). In D2 mice the number of macrophages and neutrophils in lung was increased and higher than that of B6 mice (Fig. 6), but it was ineffective to eliminate the bacteria as other bacterial infection (Wilson et al., 2007). This suggests that dysregulation of macrophages and neutrophils and dysregulation of cytokine network in D2 mice cause deficiency to remove invading bacteria. The histopathological result showed that neutrophils infiltration caused damage to the alveolar septa with the production of edema fluid during the infection. The extensive exudate formation within alveoli could further exacerbate the activity of neutrophils and macrophages.

One of the major functions of IL-17A is recruiting neutrophils to site of inflammation (Michel et al., 2007). The elevation of IL-17A levels during mycoplasma infection in D2 mice, but not B6 mice, is associated with disease pathology, including the recruitment of pulmonary neutrophils (Fig. 6B), which has been also reported in other studies (Mize et al., 2018). These results suggest that the function of IL-17A in the immune response to mycoplasma may be different based on the genetic background. The elevation of IL-17A exacerbates inflammation by recruiting neutrophils into the airways during the infection (Park et al., 2005; Okamoto Yoshida et al., 2010; Wonnemberg et al., 2016). It appears that neutrophil recruitment does not induce the recovery of mycoplasmosis, instead worsens the inflammatory response in D2 mice. Reducing inflammatory damage during mycoplasma infection by neutralizing IL-17A (Patel et al., 2013; Liu et al., 2016) could serve as a therapy to reduce lung damage during mycoplasma infection.

Our results also found that increase in LC area in MFT was one of the traits that responded to the infection. The immune cells in the LCs consist of mainly T cells and some B cells (Elewa et al., 2014). In normal B6 mice the ratio of LC area to total MFT area were significantly higher than normal D2 mice as shown in previous paper (Elewa et al., 2014) and tended to be increased as increasing the age. However, in this study we found that infected D2 mice showed the highest increase in the ratio at 14 d.p.i. In contrast, the ratio in infected B6 mice was decreased after 7 d.p.i. (Fig. 6). This result was similar to the result in murine autoimmune disease models (Elewa et al., 2015). The increase of the ratio might be caused by over expression of cytokines that induce the proliferation of immune cells in MFT area of D2 mice. For more

understanding, we should identify cell types in these LCs to elucidate their function that may be involved in the infection. However, we suspect that these cells may not give any effects or advantages to remove the pathogen but release the cytokine to activate the excessive leukocyte infiltration in the lung. Thus, further analysis should be needed to identify the type of the inflammatory cells in the LCs of these infected mice.

Finally, we performed QTL analysis to dissect genetic factors controlling the difference in infected phenotypes. However, detected QTL responsible for each phenotype was different each other (Fig. 9 and Supplementary Fig. 4). This result suggests that the difference in each phenotype is expressed under the control of respective genetic factor, indicating that many different genetic factors are present between B6 and D2 mice. However, only significant QTL was detected on chromosome 4. We have obtained a significant QTL on chromosome 4, when we performed QTL analysis for resistance or susceptibility to Sendai virus infection using body weight change as QT between B6 and D2 mice (Simon et al., 2009). Although peak position of the QTL is slightly different, it is quite interesting to hypothesize that some genetic factors on chromosome 4 may contribute to resistance or susceptibility to pathogens causing pneumonia.

In summary, we have demonstrated that D2 mice are susceptible to *M. pulmonis*, leading to the development of pneumonia, whereas B6 mice are resistant. The inability to control an effective lung defense correlates with the lack of initial bactericidal activity in D2 macrophages, indicating that lung macrophages are important factor in the first line of defense against the initial colonization. Additionally, in response to *M. pulmonis* infection, D2 mice are capable of recruiting an increased number of neutrophils to the lung, but fail to protect from the mycoplasma proliferation. These combining factors lead to an increased susceptibility as seen with increased lung colonization, neutrophil recruitment, and severe body weight loss in D2 mice. Our study showed similarity to the bacterial pneumonia and lung injury in humans. These findings could facilitate better understanding in terms of host-pathogen interaction and developing the therapeutics that minimize adverse reactions.

Acknowledgements

We thank Dr. Nobuhito Hayashimoto, Central Institute for Experimental Animals, Japan, for the stock of *M. pulmonis*, CIEA-NH strain, Dr. Norikazu Isoda, Unit of Risk Analysis and Management, Research Center for Zoonosis Control, Hokkaido University, for the assistance in cytocentrifuge, and Mr. Akio Suzuki, Laboratory of Veterinary Hygiene, Faculty of Veterinary Medicine, Hokkaido University, for the assistance in cytokine assays. Tussapon Boonyarattanasoonthorn was supported by a scholarship by the Ministry of Education, Culture, Sports, Science and Technology, Japan.

Appendix A. Supplementary data

Supplementary data to this article can be found online at <https://doi.org/10.1016/j.meegid.2019.04.019>.

References

- Boettger, C.M., Dohms, J.E., 2006. Separating mycoplasma gallisepticum field strains from nonpathogenic avian mycoplasmas. *Avian Dis.* 50, 605–607.
- Calcutt, M.J., Lysnyansky, I., Sachse, K., Fox, L.K., Nicholas, R.A.J., Ayling, R.D., 2018. Gap analysis of mycoplasma bovis disease, diagnosis and control: an aid to identify future development requirements. *Transbound. Emerg. Dis.* 65, 91–109 (00, 000–000).
- Cardona, P.J., Gordillo, S., Díaz, J., Tapia, G., Amat, I., Pallarés, Á., Vilaplana, C., Ariza, A., Ausina, V., 2003. Widespread bronchogenic dissemination makes DBA/2 mice more susceptible than C57BL/6 mice to experimental aerosol infection with mycobacterium tuberculosis. *Infect. Immun.* 71, 5845–5854.
- Cartner, S.C., Simecka, J.W., Lindsey, J.R., Cassell, G.H., Davis, J.K., 1995. Chronic respiratory mycoplasmosis in C3H/HeN and C57BL/6N mice: lesion severity and

- antibody response. *Infect. Immun.* 63, 4138–4142.
- Cartner, S.C., Simecka, J.W., Briles, D.E., Cassell, G.H., Lindsey, J.R., 1996. Resistance to mycoplasma lung disease in mice is a complex genetic trait. *Infect. Immun.* 64, 5326–5331.
- Ceola, C.F., Sampaio, J., Blatt, S.L., Cordova, C.M.M., 2016. *Mycoplasma infection* and inflammatory effects on laboratory rats bred for experimental research. *Rev. Pan-Amaz Saude* 7, 59–66.
- Chawla, S., Jena, S., Venkatsan, B., Mahara, K., Sahu, N., 2017. Clinical, pathological, and molecular investigation of mycoplasma pulmonis-induced murine respiratory mycoplasmosis in a rat (*Rattus norvegicus*) colony. *Vet. World* 10, 1378–1382.
- Chen, J., Liao, M.Y., Gao, X.L., Zhong, Q., Tang, T.T., Yu, X., Liao, Y.H., Cheng, X., 2013. IL-17A induces pro-inflammatory cytokines production in macrophages via MAPKs, NF- κ B and AP-1. *Cell. Physiol. Biochem.* 32, 1265–1274.
- Daubeuf, F., Frossard, N., 2012. Performing bronchoalveolar lavage in the mouse. *Curr. Protoc. Mouse Biol.* 2, 167–175.
- Davidson, M.K., Lindsey, J.R., Parker, R.F., Tully, J.G., Cassell, G.H., 1988. Differences in virulence for mice among strains of mycoplasma pulmonis. *Infect. Immun.* 56, 2156–2162.
- Davis, J.K., Parker, R.F., White, H., Dziedzic, D., Taylor, G., Davidson, M.K., Cox, N.R., Cassell, G.H., 1985. Strain differences in susceptibility to murine respiratory mycoplasmosis in C57BL/6 and C3H/HeN mice. *Infect. Immun.* 50, 647–654.
- Diaz, M.H., Benitez, A.J., Winchell, J.M., 2015. Investigations of mycoplasma pneumoniae infections in the United States: trends in molecular typing and macrolide resistance from 2006 to 2013. *J. Clin. Microbiol.* 53, 124–130.
- Elewa, Y.H., Bareedy, M.H., Abuel-Atta, A.A., Ichii, O., Otsuka, S., Kanazawa, T., Lee, S.H., Hashimoto, Y., Kon, Y., 2010. Structural characteristics of goat (*Capra hircus*) parotid salivary glands. *Jpn. J. Vet. Res.* 58, 121–135.
- Elewa, Y.H., Ichii, O., Otsuka, S., Hashimoto, Y., Kon, Y., 2014. Characterization of mouse mediastinal fat-associated lymphoid clusters. *Cell Tissue Res.* 357, 731–741.
- Elewa, Y.H., Ichii, O., Kon, Y., 2015. Comparative analysis of mediastinal fat-associated lymphoid cluster development and lung cellular infiltration in murine autoimmune disease models and the corresponding normal control strains. *Immunology* 147, 30–40.
- Ferreira, J.B., Yamaguti, M., Marques, L.M., Oliveira, R.C., Neto, R.L., Buzinhani, M., Timenetsky, J., 2008. Detection of mycoplasma pulmonis in laboratory rats and technicians. *Zoonoses Public Health* 55, 229–234.
- Harasawa, R., Mizusawa, H., Fujii, M., Yamamoto, J., Mukai, H., Uemori, T., Asada, K., Kato, I., 2005. Rapid detection and differentiation of the major mycoplasma contaminants in cell cultures using real-time PCR with SYBR green I and melting curve analysis. *Microbiol. Immunol.* 49, 859–863.
- Hickman-Davis, J.M., Michalek, S.M., Gibbs-Erwin, J., Lindsey, J.R., 1997. Depletion of alveolar macrophages exacerbates respiratory mycoplasmosis in mycoplasma-resistant C57BL mice but not mycoplasma-susceptible C3H mice. *Infect. Immun.* 65, 2278–2282.
- Kawai, S., Takagi, Y., Kaneko, S., Kurosawa, T., 2011. Effect of three types of mixed anesthetic agents alternate to ketamine in mice. *Exp. Anim.* 60, 481–487.
- Lai, W.C., Pakes, S.P., Bennett, M., 1996. Natural resistance to mycoplasma pulmonis infection in mice: host resistance gene(s) map to chromosome 4. *Nat. Immun.* 15, 241–248.
- Lan, Y., Chen, Z., Yang, D., Wang, X., Wang, Y., Xu, Y., Tang, L., 2016. Altered cytokine levels in bronchoalveolar lavage fluids from patients with mycoplasma pneumonia infection. *Int. J. Clin. Exp. Med.* 9, 16548–16557.
- Liu, L., Lu, J., Allan, B.W., Tang, Y., Tetreault, J., Chow, C.K., Barmettler, B., Nelson, J., Bina, H., Huang, L., Wroblewski, V.J., Kikly, K., 2016. Generation and characterization of ixekizumab, a humanized monoclonal antibody that neutralizes interleukin-17A. *J. Inflamm. Res.* 9, 39–50.
- Loganbilk, J.K., Wagner, A.M., Besselsen, D.G., 2005. Detection of mycoplasma pulmonis by fluorogenic nuclease polymerase chain reaction analysis. *Comp. Med.* 55, 419–424.
- Luehrs, A., Siegenthaler, S., Grütznert, N., Beilage, E.G., Kuhnert, P., Nathues, H., 2017. Occurrence of mycoplasma hyorhinis infections in fattening pigs and association with clinical signs and pathological lesions of enzootic pneumonia. *Vet. Microbiol.* 203, 1–5.
- Manly, K.F., Cudmore Jr., R.H., Meer, J.M., 2001. Map manager QTX, cross-platform software for genetic mapping. *Mamm. Genome* 12, 930–932.
- Michel, M.L., Keller, A.C., Paget, C., Fujio, M., Trottein, F., Savage, P.B., Wong, C.H., Schneider, E., Dy, M., Leite-de-Moraes, M.C., 2007. Identification of an IL-17-producing NK1.1(neg) iNKT cell population involved in airway neutrophilia. *J. Exp. Med.* 204, 995–1001.
- Miossec, P., Korn, T., Kuchroo, V.K., 2009. Interleukin-17 and type 17 helper T cells. *N. Engl. J. Med.* 361, 888–898.
- Mize, M.T., Sun, X.L., Simecka, J.W., 2018. Interleukin-17A exacerbates disease severity in BALB/c mice susceptible to lung infection with mycoplasma pulmonis. *Infect. Immun.* 86 (e00292–18).
- Okamoto Yoshida, Y., Umemura, M., Yahagi, A., O'Brien, R.L., Ikuta, K., Kishihara, K., Hara, H., Nakae, S., Iwakura, Y., Matsuzaki, G., 2010. Essential role of IL-17A in the formation of a mycobacterial infection-induced granuloma in the lung. *J. Immunol.* 184, 4414–4422.
- Park, H., Li, Z., Yang, X.O., Chang, S.H., Nurieva, R., Wang, Y.H., Wang, Y., Hood, L., Zhu, Z., Tian, Q., Dong, C., 2005. A distinct lineage of CD4 T cells regulates tissue inflammation by producing interleukin 17. *Nat. Immun.* 6, 1133–1141.
- Patel, D.D., Lee, D.M., Kolbinger, F., Antoni, C., 2013. Effect of IL-17A blockade with secukinumab in autoimmune diseases. *Ann. Rheum. Dis.* 72, iii116–iii123.
- Pereyre, S., Goret, J., Bébéar, C., 2016. Mycoplasma pneumoniae: current knowledge on macrolide resistance and treatment. *Front. Microbiol.* 7, 974.
- Pica, N., Iyer, A., Ramos, I., Bouvier, N.M., Fernandez-Sesma, A., García-Sastre, A., Lowen, A.C., Palese, P., Steel, J., 2011. The DBA.2 mouse is susceptible to disease following infection with a broad, but limited, range of influenza A and B viruses. *J. Virol.* 85, 12825–12829.
- Sahoo, M., Ceballos-Olvera, I., del Barrio, L., Re, F., 2011. Role of the inflammasome, IL-1 β , and IL-18 in bacterial infections. *Sci. World J.* 11, 2037–2050.
- Simon, A.Y., Moritoh, K., Torigoe, D., Asano, A., Sasaki, N., Agui, T., 2009. Multigenic control of resistance to Sendai virus infection in mice. *Infect. Genet. Evol.* 9, 1253–1259.
- Simon, A.Y., Sasaki, N., Ichii, O., Kajino, K., Kon, Y., Agui, T., 2011. Distinctive and critical roles for cellular immunity and immune-inflammatory response in the immunopathology of Sendai virus infection in mice. *Microbes Infect.* 13, 783–797.
- Sun, X., Jones, H.P., Hodge, L.M., Simecka, J.W., 2006. Cytokine and chemokine transcription profile during mycoplasma pulmonis infection in susceptible and resistant strains of mice: macrophage inflammatory protein 1 β (CCL4) and monocyte chemoattractant protein 2 (CCL8) and accumulation of CCR5⁺ Th cells. *Infect. Immun.* 74, 5943–5954.
- Sung, H., Kang, S.H., Bae, Y.J., Hong, J.T., Chung, Y.B., Lee, C.K., Song, S., 2006. PCR-based detection of mycoplasma species. *J. Microbiol.* 44, 42–49.
- Szczepanek, S.M., Majumder, S., Sheppard, E.S., Liao, X., Rood, D., Tulman, E.R., Wyand, S., Krause, D.C., Silbart, L.K., Geary, S.J., 2012. Vaccination of BALB/c mice with an avirulent mycoplasma pneumoniae P30 mutant results in disease exacerbation upon challenge with a virulent strain. *Infect. Immun.* 80, 1007–1014.
- Takahashi-Omoe, H., Omoe, K., Matsushita, S., Kobayashi, H., Yamamoto, K., 2004. Polymerase chain reaction with a primer pair in the 16S-23S rRNA spacer region for detection of mycoplasma pulmonis in clinical isolates. *Comp. Immunol. Microbiol. Infect. Dis.* 27, 117–128.
- Vogels, M.T., Mensink, E.J., Ye, K., Boerman, O.C., Verschueren, C.M., Dinarello, C.A., van der Meer, J.W., 1994. Differential gene expression for IL-1 receptor antagonist, IL-1, and TNF receptors and IL-1 and TNF synthesis may explain IL-1-induced resistance to infection. *J. Immunol.* 153, 5580–5772.
- Vogels, M.T., Eling, M.T., Otten, A., van der Meer, J.W., 1995. Interleukin-1 (IL-1)-induced resistance to bacterial infection: role of the type I IL-1 receptor. *Antimicrob. Agents Chemother.* 39, 1744–1747.
- Waites, K.B., Talkington, D.F., 2004. Mycoplasma pneumoniae and its role as a human pathogen. *Clin. Microbiol. Rev.* 17, 697–728.
- Waller, J.L., Diaz, M.H., Petrone, B.L., Benitez, A.J., Wolff, B.J., Edison, L., Tobin-D'Angelo, M., Moore, A., Martyn, A., Dishman, H., Drenzek, C.L., Turner, K., Hicks, L.A., Winchell, J.M., 2014. Detection and characterization of mycoplasma pneumoniae during an outbreak of respiratory illness at a university. *J. Clin. Microbiol.* 52, 849–853.
- Wilson, K.R., Napper, J.M., Denvir, J., Sollars, V.E., Yu, H.D., 2007. Defect in early lung defense against *Pseudomonas aeruginosa* in DBA/2 mice is associated with acute inflammatory lung injury and reduced bactericidal activity in naïve macrophages. *Microbiology* 153, 968–979.
- Wonnemberg, B., Jungnickel, C., Honecker, A., Wolf, L., Voss, M., Bischoff, M., Tschernig, T., Herr, C., Bals, R., Beisswenger, C., 2016. IL-17A attracts inflammatory cells in murine lung infection with *P. aeruginosa*. *Innate Immun.* 22, 620–625.